JOURNAL OF PROPULSION AND POWER
Vol. 16, No. 6, November–December 2000

Solid-Fuel Ramjet Regulation by Means of an Air-Division Valve

Deborah Pelosi-Pinhas* and Alon Gany†
Technion—Israel Institute of Technology, 32000 Haifa, Israel

An in-flight regulation technique, which can provide an optimal operation of a solid-fuel ramjet (SFRJ) motor over a wide flight envelope, has been analyzed. Regulation capability is essential for an efficient use of the SFRJ propulsion for applications involving variable flight and operating conditions. The method is based on a controllable air-division valve, which drives part of the inlet air into the solid-fuel port, while the rest of the airflow is channeled through a bypass to the aft-mixing section of the combustor. The model takes into account parameters influencing the burning rate of the solid fuel (e.g., port-flow rate, port diameter) and formulates a general regulation law in terms of the instantaneous opening state of the division valve for a constant fuel-to-air ratio operation. The control law was checked for certain cases, considering typical trajectories. It has demonstrated a good regulation capability over a broad operational range (between sea level and 15-km altitude).

Nomenclature

A	=	area
d	=	diameter
f	=	fuel-to-air ratio
$f(h)$	=	function of altitude in the regulation law, Eq. (22)
G	=	air mass flux
$g(M)$	=	function of Mach number in the regulation law, Eq. (23)
H	=	inlet step height
h	=	heat-transfer coefficient; altitude
L	=	fuel grain length
M	=	Mach number
m	=	temperature exponent
$\dot{m}$	=	mass-flow rate
n	=	mass-flow rate or mass flux exponent
$\dot{q}$	=	heat flux
$\dot{r}$	=	fuel regression rate
T	=	temperature; air temperature
T_0	=	stagnation air temperature
t	=	time
γ	=	specific heat ratio
ΔH_v	=	heat of gasification
ρ	=	density

Subscripts

a	=	air
b	=	bypass
c	=	combustion
f	=	fuel
in	=	inlet
max	=	maximum
min	=	minimum
nom	=	nominal
p	=	port
t	=	throat
w	=	wall

Introduction

THE solid-fuel ramjet (SFRJ) is one of the simplest airbreathing engines. The use of solid fuels in conventional engines provides many advantages: high-energy density resulting in a more compact system, simplicity (essentially, there is no need for fuel control, fuel storage and feeding systems comprising pumps and valves), safety, and easy storage. Another advantage of SFRJ motors is the high degree of combustion stability,[1] which seems to result from the mainly diffusion-controlled combustion process.

Because of their high specific impulse (3–4 times than that of solid rocket motors), SFRJ motors are particularly suitable for long-range missile and projectile propulsion at supersonic flights (typically between Mach 2 and 4); at lower Mach numbers turbojet engines with afterburner may be preferable.

Of the three types of ramjet engines—the liquid fuel ramjet, the ducted rocket, and the SFRJ, the SFRJ represents the simplest design solution because of the absence of any moving parts and the simple combustor configuration.[2] It consists of an air intake system, a combustor, and an exhaust nozzle. The combustor comprises a sudden expansion (inlet step) serving as a flame holder, an igniter, and the solid-fuel grain, often of a hollow cylinder shape (Fig. 1). Flame stabilization has been studied, e.g., by Netzer and Gany[3] and by Schulte.[4] Often flameholding limits are described on a plot of the port-to-inlet area ratio A_p/A_{in}, which is an equivalent parameter to the relative step height, determining the dimensions of the recirculation zone, vs the port-to-nozzle throat area ratio A_p/A_t, which establishes the Mach number inside the fuel port (Fig. 2). Flight conditions (Mach number and altitude) determine stagnation temperature and pressure of the incoming air to the diffuser. For a given stagnation temperature of the incoming air, any operating point (indicated by certain A_p/A_{in} and A_p/A_t ratios) above the flameholding limit enables sustained combustion, whereas points below that limit do not ensure stable operation. The figure shows that either an increase in inlet air temperature, an increase in the A_p/A_t area ratio, or an increase in the A_p/A_{in} area ratio can provide better conditions for sustained combustion. The higher the flight Mach number is, then the higher the stagnation temperature of the air, and the easier the flame stabilization.

The combustion process of the solid fuel consists of the thermal decomposition and gasification of the fuel surface because of heat transfer from the hot flow and combustion of fuel vapor with the air in the gas phase[5,6] (Fig. 1). The fuel vapor passes by diffusion and convection to the shear layer developed between the incoming airflow and the recirculation zone. In this region a part of the fuel vapor is burned with the air, and the combustion products, together with the unburned fuel vapor, flow over the solid-fuel surface downstream of the recirculation zone. From the reattachment point of the flow at the end of the recirculation zone, a turbulent boundary layer develops over the solid-fuel surface, where diffusive combustion takes place between the fuel vapor from the wall and the oxygen from the flow core.[7] The end section of the combustor usually does not contain solid fuel and is used as an aft-mixing

Received 31 August 1999; revision received 18 December 1999; accepted for publication 21 December 1999.

*Graduate Student, Faculty of Aerospace Engineering; debby@aerodyne.technion.ac.il.

†Professor and Head, Fine Rocket Propulsion Center, Faculty of Aerospace Engineering; gany@aerodyne.technion.ac.il. Associate Fellow AIAA.

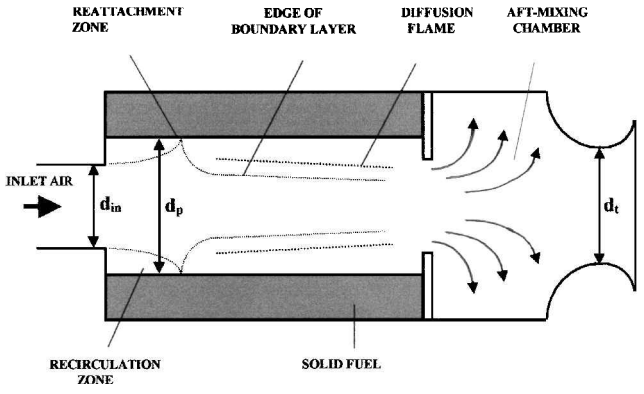

Fig. 1 Schematic of SFRJ combustor geometry and flowfield.

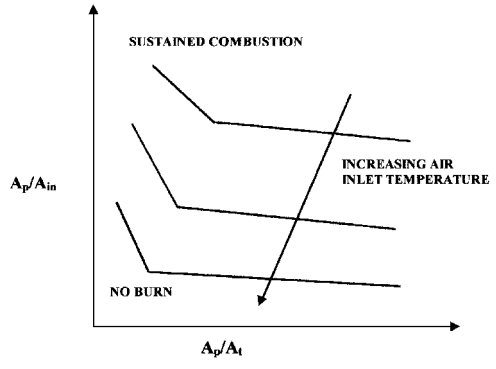

Fig. 2 Flameholding limits.

chamber in order to complete the reaction between the fuel vapors and air. Sometimes the aft-mixing chamber is fitted with a bypass air injection.

The fuel used in the SFRJ is primarily of a polymeric hydrocarbon type, e.g., polybutadiene, polyethylene, polymethylmethacrylate, providing high heat of combustion, good mechanical properties, good regression characteristics, and high combustion efficiency over a wide range of conditions. It is possible to increase both the gravimetric and the volumetric heat release of solid fuels by using certain metal additives.

In spite of the attractive features of the SFRJ motor, the use of a solid fuel complicates the internal ballistics and the design of a desired working point, as there is no direct control on the fuel flow rate. The fuel regression rate is known to be dominated by the heat transfer to the fuel surface and the fuel gasification process. Thus, it depends on physical and chemical properties of the matter, on the incoming airflow rate, and on the geometry (basically the diameter) of the combustion chamber.[8,9] To ensure effective motor operation over a wide flight envelope, it is necessary to control the combustion process, allowing motor operation at optimal conditions over the desirable operating range. Such an optimal operation requirement can be, for instance, the motor capability of operating at a constant, desirable fuel-to-air ratio, over a wide range of flight conditions. This requires the regulation of the fuel mass-flow rate during flight because of changes in the air mass-flow rate due to the variable flight conditions (altitude and Mach number) as well as the increase in fuel port diameter caused by solid fuel burning. A higher flight velocity or a lower altitude both increase the air mass-flow rate, causing a reduction of the fuel-to-air ratio, which may affect motor performance significantly. The increase in the fuel port diameter with time also reduces fuel-to-air ratio by diminishing the fuel mass-flow rate.

SFRJ motors do have some self-throttling characteristics that enable them to partially overcome this problem: the dependence of fuel regression rate on airflow rate and temperature implies that at lower flight altitudes, which are characterized by higher flow rates and stagnation temperatures of the incoming air, the fuel flow rate

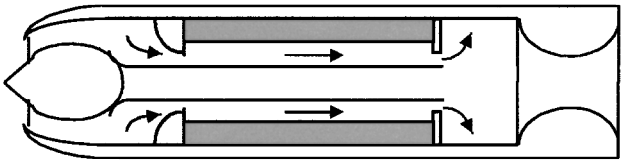

a) Entire amount of air flows through the port

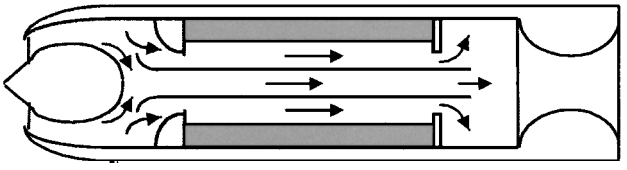

b) Air is divided to the port and the tube

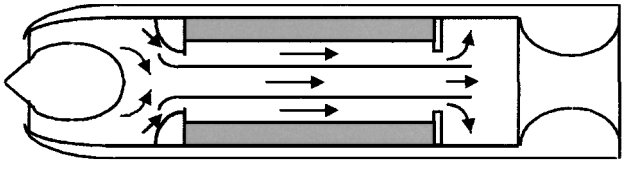

c) Most of the air flows through the tube

Fig. 3 Tube-in-hole technique.[11]

increases as well and vice-versa. However, this self-throttling characteristic of the SFRJ is not complete in itself, and additional suitable methods for the control of fuel mass-flow rate should be applied. This control can be achieved either by a controlled spillage of part of the inlet air or by a regression-rate control of the fuel. The first method has been adopted in many operating systems other than the SFRJ (e.g., YF-12 and Concord aircraft use spillage control of inlet air). The method consists of spilling a required quantity of inlet air into the atmosphere, without entering the combustor. The second method seeks fuel regression-rate control by varying the effective air mass-flow rate over the fuel surface. The tube-in-hole method, originally proposed for enhancing flame stabilization in the SFRJ at high airflow rate regimes,[1,10] can be used for regression-rate control. This method uses a tube coaxially placed in the grain port hole (Fig. 3). The tube divides the inlet air into two parts: one is directed into the annular passage over the fuel surface, and the other flows through the central tube directly to the aft end. In the first position (Fig. 3a) the entire amount of air flows through the annular passage producing the highest regression rate; in the second position (Fig. 3b) the tube splits the airflow, and the air mass-flow rate over the fuel surface is reduced, producing a lower regression rate. In the third position (Fig. 3c) most of the air flows through the tube, and only the least amount of air necessary for sustained combustion is directed into the fuel port producing the lowest regression rate. Krishnan and George[11] conducted recently a parametric study adopting the tube-in-hole method for certain typical configurations of SFRJ gun-launched projectiles, varying fuel grain lengths, inlet diameters, and launch angles.

The objective of the present work is to propose and investigate the possibility of regulating the SFRJ operation and to determine the effectiveness of such a regulation over a wide range of flight conditions. The work focuses on a method that seems to offer good control capabilities. This method is based on an air-division valve,[12] which divides the incoming airflow from the diffuser into two separate flows (Fig. 4); a part of the air (the principal airflow) is drawn directly into the combustion chamber through the port of the solid-fuel grain and determines the fuel flow rate, while the other part (the bypass airflow) flows through a bypass to the aft-mixing section of the combustion chamber, determining the overall fuel-to-air ratio.

An analytical study has been conducted, formulating a general regulation law for the air-division valve.

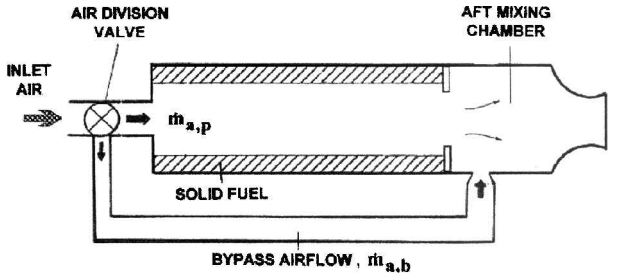

Fig. 4 Schematic description of the combustion chamber showing the air-division valve concept.

Analysis

Fuel Regression Rate

Being a result of thermal degradation and gasification of the solid fuel,[13,14] the regression rate of a typical polymeric SFRJ fuel is proportional to the heat flux to the surface according to

$$\dot{r} = \dot{q}_w / \rho_f \Delta H_v \propto \dot{q}_w \tag{1}$$

Following is a model characterizing the average fuel regression rate, using physical approximations, as justified by Hadar and Gany.[13] For a relatively high activation energy of the polymer decomposition process, the fuel regression is a quasi-equilibrium process, with a practically constant value of the heat of gasification. The heat-transfer mechanism is assumed to be dominated by forced convection through the turbulent boundary layer. The heat flux to the fuel surface is

$$\dot{q}_w = h(T_c - T_w) \tag{2}$$

As a first approximation, both the wall temperature and the diffusion flame temperature can be assumed more or less constant, hence

$$\dot{q}_w \propto h \tag{3}$$

In a developed turbulent boundary layer the heat-transfer coefficient can be expressed by Reynolds analogy. Under such conditions it can be correlated in terms of the air mass flux through the port G and the port diameter d:

$$h \propto G^{0.8} d^{-0.2} \tag{4}$$

where

$$G = \frac{\dot{m}_{a,p}}{(\pi d^2/4)} \tag{5}$$

For noncircular fuel ports one can obtain similar expressions by substituting the hydraulic diameter for the port diameter.

Substituting Eqs. (1) and (3) in Eq. (4) and generalizing the power law, one obtains

$$\dot{r} \propto G^n d^{n-1} \tag{6}$$

In terms of the mass-flow rate through the port (or the principal airflow rate), Eq. (6) becomes

$$\dot{r} \propto \dot{m}_{a,p}^n d^{-(1+n)} \tag{7}$$

An additional parameter that can be taken into account is the total temperature of the incoming air T_0, which is known to influence fuel regression rate. The more comprehensive model can then include this effect:

$$\dot{r} \propto \dot{m}_{a,p}^n d^{-(1+n)} T_0^m \tag{8}$$

where the total air temperature can be expressed in terms of flight Mach number and ambient air temperature T (depending on flight altitude):

$$T_0 = T \cdot \{1 + [(\gamma - 1)/2]M^2\} \tag{9}$$

The fuel regression-rate model as presented here gives a general scheme that can be replaced by test data or other correlations [see, for example, Ref. 12 for hydroxil-terminated polybutadiene (HTPB)].

Air-Division Valve Concept

Using an air-division valve, the incoming air can be divided into two parts prior to entering the combustor: the principal (port) airflow and the bypass airflow (see Fig. 4), where

$$\dot{m}_a = \dot{m}_{a,p} + \dot{m}_{a,b} \tag{10}$$

The airflow division concept is based on the fact that the fuel mass-flow rate is directly dependent on the principal airflow rate, which flows through the fuel port, and is independent of the overall airflow rate coming through the diffuser. On the other hand, the overall fuel/air ratio f is related to the overall incoming airflow $\dot{m}_a$:

$$f = \frac{\dot{m}_f}{\dot{m}_a} = \frac{\dot{m}_f}{\dot{m}_{a,p} + \dot{m}_{a,b}} \tag{11}$$

It is possible to find a relation between the fuel mass-flow rate and the principal (port) airflow rate, which enables us to control the fuel-to-air ratio via regulating the port-to-overall airflow rate ratio $\dot{m}_{a,p}/\dot{m}_a$. For a single port, cylindrical combustion chamber, the fuel mass-flow rate is determined as follows:

$$\dot{m}_f = \pi d \rho_f L \dot{r} \tag{12}$$

For a given fuel grain length (and a constant fuel density)

$$\dot{m}_f \propto d \cdot \dot{r} \tag{13}$$

Making use of Eq. (8), the fuel mass-flow rate can be expressed as a function of the principal airflow rate, the port diameter, and the total temperature:

$$\dot{m}_f \propto (\dot{m}_{a,p}/d)^n \cdot T_0^m \tag{14}$$

Control Law

Regulation of the SFRJ operation can be very significant, particularly for maintaining a desirable performance level in typical variable ambient, flight, and operating conditions encountered by the motor. As just mentioned, the present work defines the desirable operating state as motor operation at constant fuel-to-air ratio. However, different requirements can be easily handled, yielding similar regulation models. To fulfill this requirement, a control law is derived based on controlled variation of the port-to-overall airflow ratio.

Nominal conditions are defined, at which a nominal value of fuel burning rate and a desirable nominal value of fuel-to-air ratio exist. The fuel-to-air ratio at any point in the flight envelope is compared to the nominal, desirable ratio:

$$f = f_{\text{nom}} \tag{15}$$

After substituting the fuel mass-flow rate expression from Eq. (14) in the fuel-to-air ratios f and f_{nom} in Eq. (15), the following control law is derived, correlating the instantaneous opening state of the division valve as a function of air mass-flow rate, air stagnation temperature, and port diameter, relative to the nominal values:

$$\frac{\dot{m}_{a,p}}{\dot{m}_a} \propto \left(\frac{\dot{m}_{a,p}}{\dot{m}_a}\right)_{\text{nom}} \cdot \left(\frac{d}{d_{\text{nom}}}\right) \cdot \left(\frac{\dot{m}_a}{\dot{m}_{a,\text{nom}}}\right)^{[(1-n)/n]} \cdot \left(\frac{T_0}{T_{0,\text{nom}}}\right)^{-(m/n)} \tag{16}$$

The port diameter increases as the fuel grain is burned:

$$d = d_{\min} + \int_0^t 2\dot{r}\, \mathrm{d}t \tag{17}$$

where the fuel regression rate can be expressed in the following form:

$$\dot{r} \propto \dot{m}_{a,p}^n d^{-(1+n)} \cdot T_0^m \propto (\dot{m}_{a,p}/\dot{m}_a)^n \cdot \dot{m}_a^n \cdot d^{-(1+n)} \cdot T_0^m \tag{18}$$

The burning rate can now be related to the nominal conditions

$$\dot{r} = \dot{r}_{\text{nom}} \cdot \frac{(\dot{m}_{a,p}/\dot{m}_a)^n}{(\dot{m}_{a,p}/\dot{m}_a)^n_{\text{nom}}} \cdot \left(\frac{\dot{m}_a}{\dot{m}_{a,\text{nom}}}\right)^n \cdot \left(\frac{d}{d_{\text{nom}}}\right)^{-(1+n)} \cdot \left(\frac{T_0}{T_{0,\text{nom}}}\right)^m \tag{19}$$

Assuming that the air capture area is constant (critical or supercritical inlet operation), the air mass-flow rate varies with flight Mach number and altitude according to

$$\dot{m}_a \propto \rho \cdot M \cdot T^{\frac{1}{2}} \tag{20}$$

Making use of Eqs. (16) and (20), one can express the control law in a more general form as a function of flight conditions (Mach number and altitude) and the port diameter:

$$\dot{m}_{a,p}/\dot{m}_a \propto (\dot{m}_{a,p}/\dot{m}_a)_{\text{nom}} \cdot (d/d_{\text{nom}}) \cdot f(h) \cdot g(M) \tag{21}$$

where $f(h)$ and $g(M)$ are functions of the altitude and Mach number, respectively:

$$f(h) = \left(\frac{\rho}{\rho_{\text{nom}}}\right)^{[(1-n)/n]} \cdot \left(\frac{T}{T_{\text{nom}}}\right)^{[(1-n-2m)/2n]} \tag{22}$$

$$g(M) = \left(\frac{M}{M_{\text{nom}}}\right)^{[(1-n)/n]} \cdot \left[\frac{1+[(\gamma-1)/2]M^2_{\text{nom}}}{1+[(\gamma-1)/2]M^2}\right]^{(m/n)} \tag{23}$$

The nominal opening state of the division valve takes into account the most extreme conditions over the operating envelope, where the entire amount of air should flow through the fuel port (i.e., $\dot{m}_{a,p}/\dot{m}_a = 1$). Hence,

$$(\dot{m}_{a,p}/\dot{m}_a)_{\text{nom}} = 1/\{(d/d_{\text{nom}})_{\max} \cdot [f(h)]_{\max} \cdot [g(M)]_{\max}\} \tag{24}$$

Results

Regulation of an SFRJ motor by means of the air-division valve, using the control law [Eq. (24)] that ensures operation at a constant optimal fuel-to-air ratio at any point over the operating envelope, has been studied via some examples of typical trajectories. Numerical solutions have been found for a flight envelope comprising a 0- to 15-km altitude range and Mach numbers from 2 to 3. The fuel grain was assumed to have internal and external diameters of 80 and 160 mm, respectively.

The opening state of the valve represented by the mass airflow rates ratio $\dot{m}_{a,p}/\dot{m}_a$ has been determined as a function of time for two representative trajectories: a linear climbing from sea level to 15 km and a linear descent from 15 km to sea level, both at a constant Mach number ($M = 2.5$) flight.

Nominal conditions have been established as follows: the nominal flight altitude is sea level, the nominal Mach number is $M = 2.5$, and the nominal port diameter is the initial fuel port diameter. Figures 5–8 show the behavior of the functions $f(h)$ and $g(M)$ under such conditions. Changes in the n and m exponents influence, sometimes significantly, the maximal value of the functions, which is taken into account in the calculation of the nominal opening state of the valve. The $f(h)$ function behavior changes significantly for both n and m parameters variation (Figs. 5 and 7), whereas the $g(M)$ function is influenced only by the temperature m exponent change (Fig. 8) and is almost not affected by a change in the n exponent (Fig. 6).

A parametric study has been conducted, varying initial fuel port diameter as well as the exponents n and m (characterizing fuel regression rate), keeping a constant external fuel diameter (160 mm).

Because of the linear influence of the port diameter on the mass airflow rates ratio [Eq. (21)], the changes in the opening state of the valve are significantly reduced as the initial port diameter is increased. Yet, even with the smallest initial port diameter (80 mm), the regulation can be applied successfully in both trajectories, linear climbing (Fig. 9) and linear descent (Fig. 10).

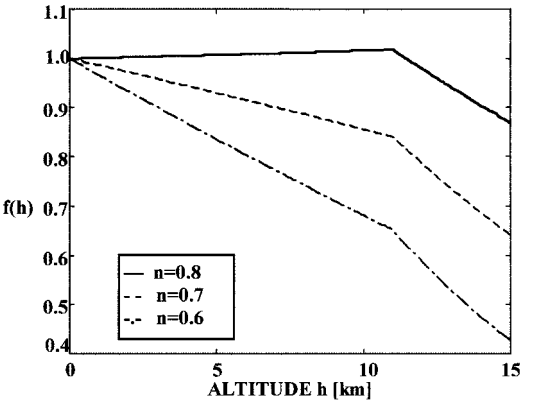

Fig. 5 $f(h)$ **function of altitude for different** n **values with** $m = 1$.

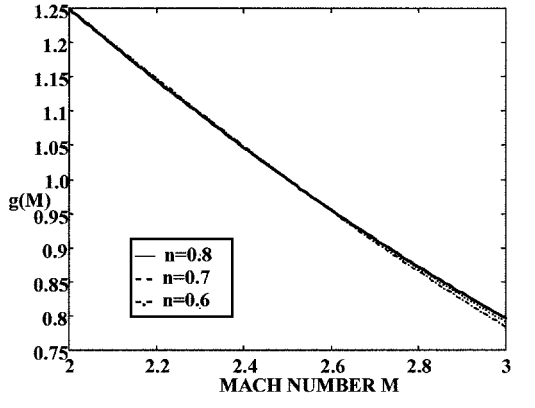

Fig. 6 $g(M)$ **function of Mach number for different** n **values with** $m = 1$.

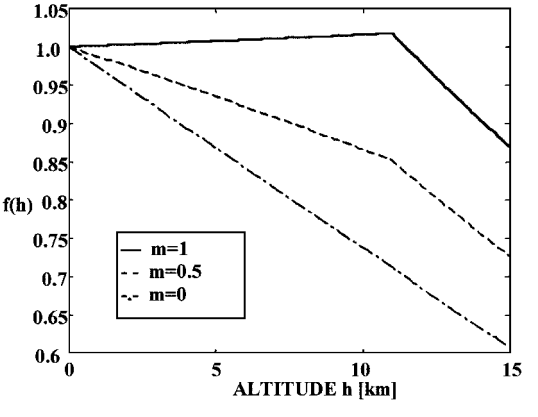

Fig. 7 $f(h)$ **function of altitude for different** m **values with** $n = 0.8$.

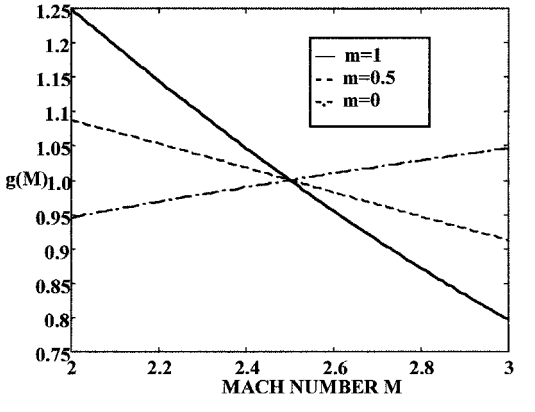

Fig. 8 $g(M)$ **function of Mach number for different** m **values with** $n = 0.8$.

The following cases relate to the nominal fuel grain dimensions.

Figures 11 and 12 show the mass airflow rates ratio as a function of time for different values of m (indicating the temperature influence) with the given value of $n = 0.8$. The variation of the m power has a minor effect on the results: in the climbing case (Fig. 11) temperature influence enhances regulation needs. A smaller m would thus be preferable. In the descent case (Fig. 12) the temperature influence improves the situation of motor operation, implying a higher initial airflow rates ratio and reduced regulation needs.

Figures 13 and 14 show the mass airflow rates ratio as a function of time for different values of n (characterizing mass-flow effect on fuel regression rate) with a similar influence of temperature ($m = 1$).

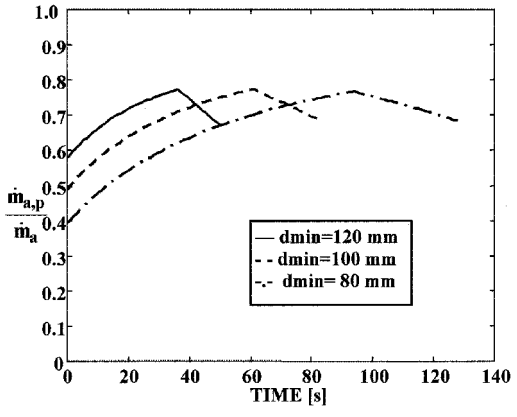

Fig. 9 Mass airflow rates ratio as a function of time for different initial port diameters at constant Mach number (M = 2.5) flight and linear climbing from sea level to 15 km (n = 0.8 and m = 1).

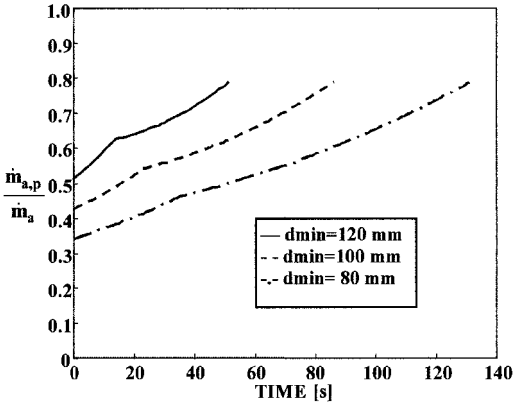

Fig. 10 Mass airflow rates ratio as a function of time for different initial port diameters at constant Mach number (M = 2.5) flight and linear descent from 15 km to sea level (n = 0.8 and m = 1).

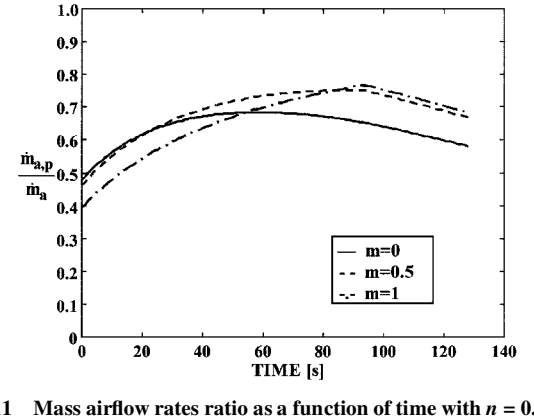

Fig. 11 Mass airflow rates ratio as a function of time with n = 0.8 and different m values for constant Mach number (M = 2.5) flight and linear climbing from sea level to 15 km.

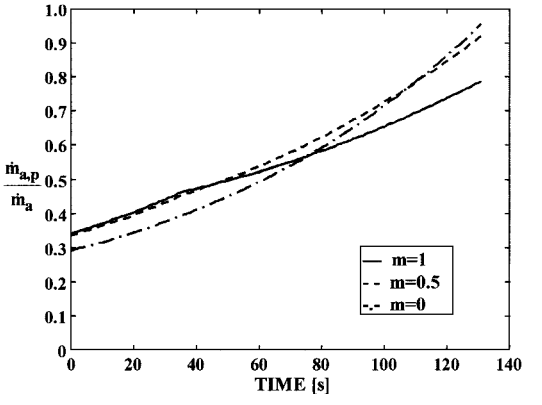

Fig. 12 Mass airflow rates ratio as a function of time with n = 0.8 and different m values for constant Mach number (M = 2.5) flight and linear descent from 15 km to sea level.

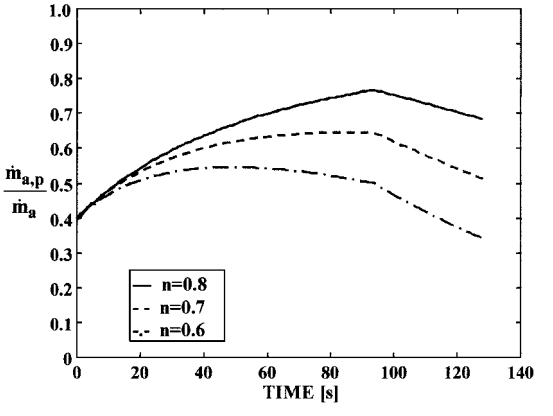

Fig. 13 Mass airflow rates ratio as a function of time with m = 1 and different n values for constant Mach number (M = 2.5) flight and linear climbing from sea level to 15 km.

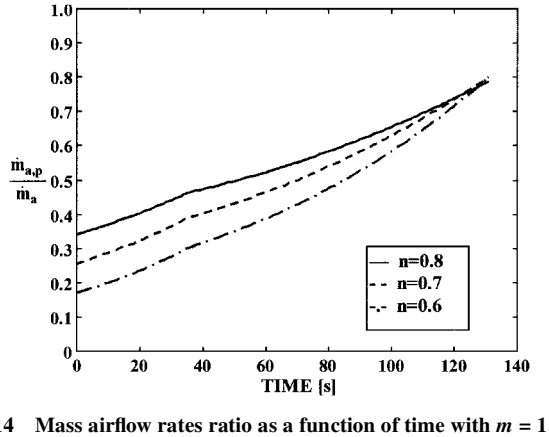

Fig. 14 Mass airflow rates ratio as a function of time with m = 1 and different n values for constant Mach number (M = 2.5) flight and linear descent from 15 km to sea level.

A reduction in the n power causes a reduction in the opening state of the valve. This is characterized by reduced airflow rates ratio variations (or reduced regulation needs) for the constant Mach-number climbing case (Fig. 13) and by a significant decrease of the initial opening state of the valve for the constant Mach-number descent case (Fig. 14), which may represent the most critical situation. In fact, at high altitudes where the air density decreases, implying a reduction in the incoming air mass-flow rate, the predicted initial small airflow rates ratio in the descent case (Fig. 14) would imply very fuel-rich combustor operation along the fuel port section in addition to relatively low chamber pressures. Combustor behavior under such an extreme situation should be checked experimentally

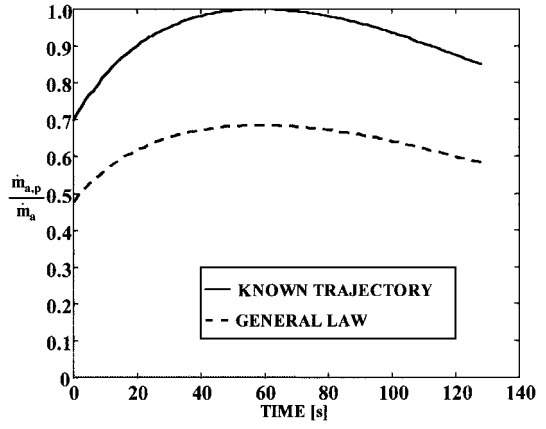

Fig. 15 Mass airflow rates ratio as a function of time (with $n = 0.8$ and $m = 0$) for constant Mach number ($M = 2.5$) flight and linear climbing from sea level to 15 km.

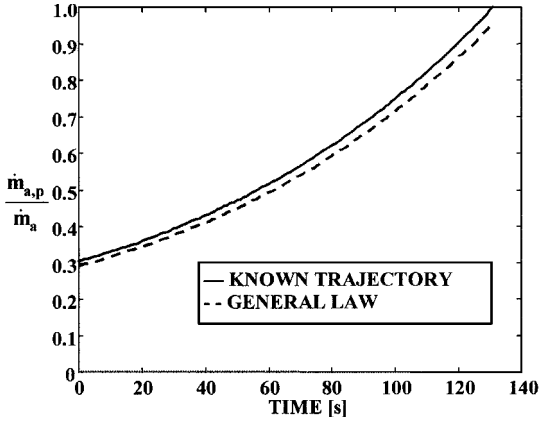

Fig. 16 Mass airflow rates ratio as a function of time (with $n = 0.8$ and $m = 0$) for constant Mach number ($M = 2.5$) flight and linear descent from 15 km to sea level.

in order to ensure that no motor extinction takes place and that sustained flame within the combustor along with effective regulation can be maintained.

In addition to the general case, the regulation law was applied to the same climbing and descent examples, when the trajectories and the flight characteristics were known a priori (Figs. 15 and 16). In such cases the mass airflow rates ratio is determined optimally so that the opening capability of the valve is fully exploited. This can be observed particularly in the climbing trajectory case (Fig. 15). Of course, such a situation is better than the former cases (Figs. 13 and 14), where nonpreceding information on the trajectory implies only partial use of the valve opening range capability.

Conclusions

An SFRJ regulation by means of an air-division valve has been modeled and analyzed yielding a regulation law for a fixed fuel-to-air ratio. It has been demonstrated that the opening state of the valve can be successfully determined at any operating point during flight or calculated a priori (if the trajectory is known) enabling optimal motor operation at a desirable constant fuel-to-air ratio. As long as the principal airflow is enough to sustain the flame, the use of the regulation law seems to offer good control capabilities over a wide operation range. The general model comes to demonstrate the feasibility of the regulation concept; the regulation law should be adapted to specific cases (given the nature of the mission and motor configuration) to provide a more detailed design prediction.

The present research provides a predictive model to determine the regulation needs at any point over the flight envelope. Nevertheless, the air-division valve concept can also be used in a closed-loop control, where the motor state is monitored by signals received, e.g., from pressure and temperature gauges.

Acknowledgment

Presented as Paper ISABE 99-7245, 14th International Symposium on Airbreathing Engines, Florence, Italy, 5–10 September 1999.

References

[1]"Solid Fuel Ramjet," United Technologies Chemical Systems, San Jose, CA, 1980, pp. 12–14.

[2]Timnat, Y. M., "Recent Developments in Ramjets, Ducted Rockets and Scramjets," *Progress in Aerospace Science*, Vol. 27, No. 3, 1990, pp. 201–235.

[3]Netzer, A., and Gany, A., "Burning and Flameholding Characteristics of a Miniature Solid Fuel Ramjet Combustor," *Journal of Propulsion and Power*, Vol. 7, No. 3, 1991, pp. 357–363.

[4]Schulte, G., "Fuel Regression and Flame Stabilization Studies of Solid-Fuel Ramjets," *Journal of Propulsion and Power*, Vol. 2, No. 4, 1986, pp. 301–304.

[5]Netzer, D. W., "Model Applications to Solid-Fuel Ramjet Combustion," *Journal of Spacecraft and Rockets*, Vol. 15, No. 5, 1978, pp. 263, 264.

[6]Zvuloni, R., Gany, A., and Levy, Y., "Geometric Effects on the Combustion in Solid Fuel Ramjets," *Journal of Propulsion and Power*, Vol. 5, No. 1, 1989, pp. 32–36.

[7]Stevenson, C. A., and Netzer, D. W., "Primitive-Variable Model Applications to Solid-Fuel Ramjet Combustion," *Journal of Spacecraft and Rockets*, Vol. 18, No. 1, 1981, pp. 89–94.

[8]Mady, C. J., Hickey, P. J., and Netzer, D. W., "Combustion Behavior of Solid-Fuel Ramjets," *Journal of Spacecraft and Rockets*, Vol. 15, No. 3, 1978, pp. 131, 132.

[9]Netzer, D. W., "Modeling Solid-Fuel Ramjet Combustion," *Journal of Spacecraft and Rockets*, Vol. 14, No. 12, 1977, pp. 762–766.

[10]Keirsey, J. L., "Solid Fuel Ramjet Flow Control Device," U.S. Patent 628,688, 1986.

[11]Krishnan, S., and George, P., "Solid Fuel Ramjet Combustor Design," *Progress in Aerospace Science*, Vol. 34, No. 4, 1998, pp. 219–256.

[12]Leisch, S., and Netzer, D. W., "Solid Fuel Ramjets," *Tactical Missile Propulsion*, edited by G. E. Jensen and D. W. Netzer, Vol. 170, Progress in Astronautics and Aeronautics, AIAA, Reston, VA, 1996, Chap. 13, pp. 469–496.

[13]Hadar, I., and Gany, A., "Fuel Regression Mechanism in a Solid Fuel Ramjet," *Propellants, Explosives, Pyrotechnics*, Vol. 17, No. 3, 1992, pp. 70–76.

[14]Ben-Arosh, R., and Gany, A., "Similarity and Scale Effects in Solid-Fuel Ramjet Combustors," *Journal of Propulsion and Power*, Vol. 8, No. 3, 1992, pp. 615–623.